Progress In Electromagnetics Research C, Vol. 25, 27–40, 2012

EXPERIMENTAL RESULTS ON HIPERLAN/2 ANTENNAS FOR WEARABLE APPLICATIONS

S. Sankaralingam* and B. Gupta

Department of Electronics and Tele-Communication Engineering, Jadavpur University, Kolkata 700032, India

Abstract—This paper addresses the design and development of HiperLAN antennas meeting the IEEE 802.11a standards for wearable applications. Five such antennas are investigated for their performance characteristics, out of which three are conventional copper based antennas and the remaining two are fully fabric antennas. The results reveal that all the proposed antennas are suitable for HiperLAN applications yielding antenna gain in the order of 7–11 dBi. This study demonstrates that fully fabric antennas outperform the copper based antennas.

1. INTRODUCTION

Communications on the human body is a relatively unexplored commodity for the personal and mobile communications community. The military and the special services, such as fire-fighters, have been using on-body systems to support their users in various hazardous environments. A wearable antenna is an essential subsystem of any body-centred Wireless LAN and therefore it plays a paramount role in optimal design of any wearable system. The Wireless LAN devices use the following ISM wavebands according to the IEEE 802.11 standards:

- Bluetooth 2450 MHz (IEEE 802.11b).
- Hiper LAN 5800 MHz (IEEE 802.11a).

Bluetooth ISM band ranges from 2400 MHz–2485 MHz. Bluetooth technology is aimed for short-range communication between all kinds of wireless devices within a range of 10 m. HiperLAN technology operates in the 5 GHz frequency band using Orthogonal Frequency Division Multiplexing (OFDM) and offers many features like high

Received 27 August 2011, Accepted 14 October 2011, Scheduled 24 October 2011
* Corresponding author: S. Sankaralingam (slingam.nec@gmail.com).

speed data transmission (up to 54 Mbps), security support, mobility support and increased range upto 50 m. HiperLAN/2 band ranges from 5725 MHz–5875 MHz. For the wireless body-centric network to be accepted by the public, wearable antennas need to be hidden and of low profile. This requires a possible integration of these systems within everyday clothing. Microstrip patch is a suitable candidate for any wearable application, as it can be made conformal for integration into clothing [1–3]. The aim of this paper is to design, develop and test the performance characteristics of body-centric microstrip HiperLAN antennas for ISM applications. Five antennas are considered — three copper based and two fully fabric antennas. The impedance characteristics of all the five antennas are studied and the radiation characteristics of one copper based and one fully fabric antennas are tested. All the five investigated antennas yield satisfactory results.

2. DESIGN AND DEVELOPMENT OF ANTENNAS

2.1. Design Aspects

The copper based antennas make use of copper for all their conducting parts whereas the fully fabric antennas utilize Zelt conductive fabric. Zelt fabric is more durable, tear resistant and can conform to any shape. It can be cut and sewn like ordinary fabric to make protective clothing. The surface resistivity of Zelt is 0.01 ohms/sq and it can withstand temperature up to 70°C. Its thickness is 0.1613 mm. In all the five cases of antennas, the polyester fabric is used as the dielectric substrate material. The value of dielectric constant of polyester fabric is 1.44 as measured by a novel technique proposed in [4] by the authors of this manuscript. The design specifications of all the five antennas and the geometry used in each case are tabulated in Table 1. The detailed design procedure for a rectangular microstrip antenna is outlined in [5, 6] and that for circular antenna in [7, 8]. The steps involved in the design of a triangular patch antenna are listed in [9].

2.2. Modelling and Fabrication of Antennas

Modeling of antennas is performed using Method of Moments (MoM) based IE3D simulator [10] from Zeland Software Inc., USA. An infinite ground plane is assumed in the simulation so as to avoid back lobes in the radiation patterns whereas the dimensions of the ground plane in the fabricated antennas are taken as 120 mm × 120 mm. The thicknesses of top signal layer and bottom ground plane are 0.1 mm and 0.5 mm respectively in the case of copper based antennas (1–3). The patch and ground plane of the antennas (1–3) are cut using CNC

Table 1. Design specifications of various antennas developed.

Design parameter	**Copper based**			**Electro-textile based**	
	Antenna 1	**Antenna 2**	**Antenna 3**	**Antenna 4**	**Antenna 5**
Geometry	Rectangular	Circular	Triangular	Rectangular	Circular
Resonant frequency(GHz)	5.8	5.8	5.8	5.8	5.8
Substrate dielectric constant	1.44	1.44	1.44	1.44	1.44
Substrate thickness (mm)	2.85	2.85	2.85	2.85	2.85
Loss tangent of the substrate	0.01	0.01	0.01	0.01	0.01
Material used for ground plane	Copper	Copper	Copper	Zelt	Zelt
Material used for patch	Copper	Copper	Copper	Zelt	Zelt

machine so that the accuracy is about 20 μm. Electro-textile based antennas (4 and 5) use Zelt fabric for both patch and ground plane whose thickness is 0.1613 mm. Here again, the size of the ground plane is 120 mm × 120 mm for antennas 4 and 5. The size of the insulating fabric material in each case of the antenna is equal to that of ground plane. These insulating fabric pieces are stacked and stitched properly to get required thickness. While assembling the antenna elements, the copper sheets are just fixed on the dielectric fabric material with scotch tape and due care is taken such that there is no air gap between the insulating fabric material and the conducting parts of the antenna. While assembling the fabric materials for making antennas 4 and 5, conducting threads may be used for stitching. While modeling the coaxial probe feed to patch, the inner and outer diameters of the probe are taken as 1.3 mm and 4.1 mm respectively corresponding to standard 50 ohm SMA connector. A shorting pin of 1.0 mm diameter is connected at the centre of circular patch in order to suppress higher order modes. The dimensions of rectangular antennas 1 and 4 are length = 19.3 mm and width = 23.41 mm. The designed value of radius of each of the circular radiating patches (antennas 2 and 5) is 11.4 mm. The side length of the triangular radiating patch (antenna 3) under investigation is 25.5 mm. The feed position is optimized to get good matching characteristics (50 ohm impedance) at the center

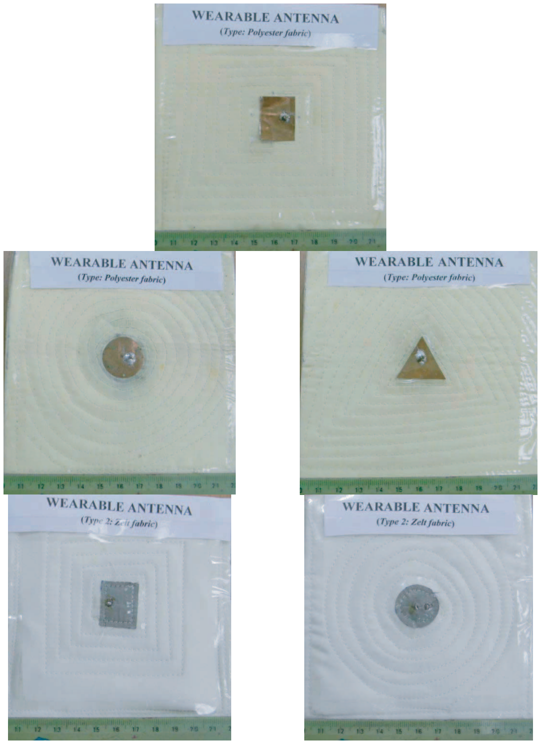

Figure 1. Photographs of HiperLAN antennas.

frequency. The optimized feed position for antennas 1 and 4 are 5.4 mm from the centre of the patch along the length direction. In case of antennas 2 and 5, they are positioned at a radial distance of 4.5 mm and 5.4 mm respectively, from the centre of circular patch. For antenna 3, it is located at a distance of 3.7 mm from the centroid of triangular shaped patch towards its apex. The photographs of all these fabricated HiperLAN antennas are shown in Fig. 1.

3. IMPEDANCE CHARACTERISTICS

3.1. Simulated and Measured Results

Simulations and measurements are carried out over the frequency range of 5.2 GHz to 6.2 GHz for all five antennas 1–5 developed. Fig. 2 shows simulated and measured S_{11} plots of HiperLAN antenna (# 1) with rectangular geometry. As depicted by these simulation results, this wearable antenna resonates at a frequency of 5.84 GHz

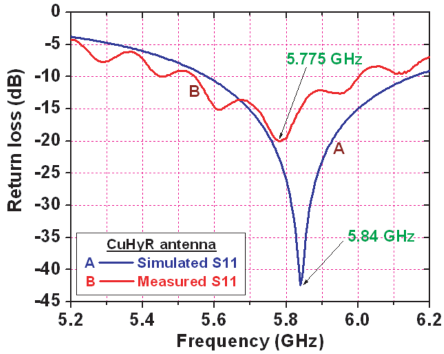

Figure 2. Return loss characteristics of antenna 1.

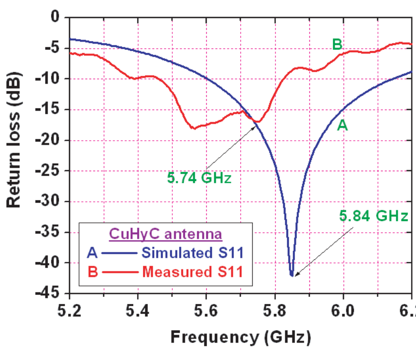

Figure 3. Return loss plot of antenna 2.

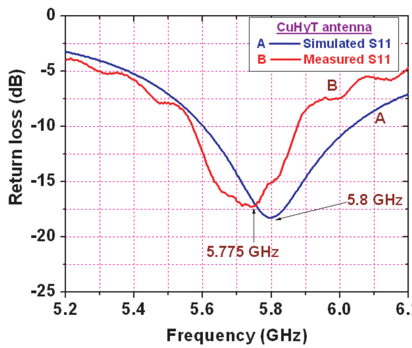

Figure 4. Return loss plot of antenna 3.

and exhibits a -10 dB return loss bandwidth of 574.85 MHz. Fig. 3 corresponds to simulated and measured return loss characteristics of the wearable HiperLAN antenna (# 2) with circular geometry. This figure reveals that the simulated values of resonant frequency and impedance bandwidth of the antenna are 5.84 GHz and 539.72 MHz respectively. Referring to Fig. 4, it is seen that the triangular microstrip HiperLAN antenna (# 3) is simulated at a resonant frequency of 5.8 GHz with an impedance bandwidth of 432.76 MHz. The measurements are done using a vector network analyzer (Model # 5071 B) from Agilent Technologies. Before measuring the impedance parameters of the antennas under investigation, the network analyzer is calibrated using the 2 port Ecal module [11], bearing model # 85092C for an operating frequency ranging from 5.2 GHz to 6.2 GHz, which

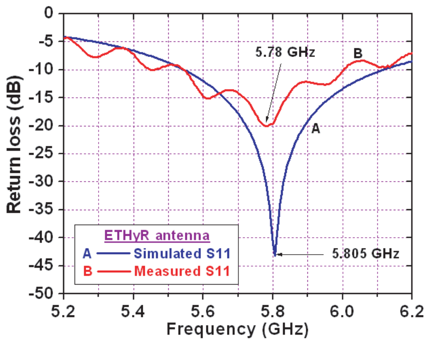

Figure 5. S_{11} plot of antenna 4.

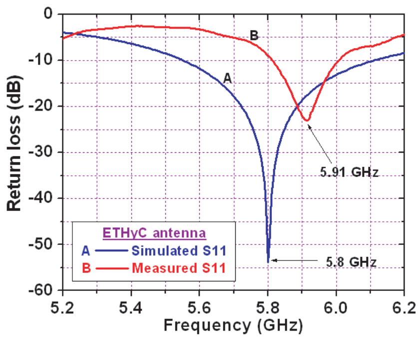

Figure 6. S_{11} plot of antenna 5.

provides excellent accuracy. Fabricated antenna (# 1) structure is measured for a resonant frequency of 5.775 GHz with an impedance bandwidth of 455.4 MHz having a return loss of −20.12 dB at the resonant frequency as shown in Fig. 2. Measured quantities of resonant frequency and impedance bandwidth of antenna (# 2) are 5.74 GHz and 360 MHz respectively. Triangular microstrip antenna (# 3) resonates at 5.775 GHz (return loss −17.76 dB) and yields an impedance bandwidth of 308.7 MHz as depicted in Fig. 4.

Figure 5 shows simulated and measured S_{11} plots of electro-textile HiperLAN antenna (# 4) with rectangular geometry. As depicted by these simulation results, this wearable antenna resonates at a frequency of 5.805 GHz and exhibits a −10 dB return loss bandwidth of 571.82 MHz. Fig. 6 corresponds to simulated and measured return loss characteristics of wearable HiperLAN antenna (# 5) with circular geometry. This figure reveals that the simulated values of resonant frequency and impedance bandwidth of antenna are 5.8 GHz and 558.6 MHz respectively. Fabricated antenna (# 4) structure is measured for a resonant frequency of 5.78 GHz with an impedance bandwidth of 292 MHz having a return loss of −17.17 dB at the resonant frequency as shown in Fig. 5. Measured quantities of resonant frequency and impedance bandwidth of antenna (# 5) are 5.91 GHz and 353 MHz respectively with a return loss of −20.85 dB (Fig. 6).

3.2. Discussions

Measured results are tabulated in Table 2 along with the corresponding theoretical predictions for all five antennas studied. The deviation between simulated and measured resonant frequencies is 1.1% in case of antenna 1; 1.71% and 0.0043% in case of antennas 2 and 3

Table 2. Impedance characteristics of wearable antennas in HiperLAN band.

Name of the antenna	Resonant frequency (GHz)		Impedance bandwidth (MHz)	
	Simulated	Measured	Simulated	Measured
Rectangular antenna (# 1)	5.84	5.775	574.85	455.4
Circular antenna (# 2)	5.84	5.74	539.72	360.0
Triangular antenna (# 3)	5.80	5.775	432.76	308.7
Rectangular antenna (# 4)	5.805	5.78	571.82	292
Circular antenna (# 5)	5.8	5.91	558.6	353

respectively. Among these three antennas, triangular patch antenna (# 3) shows an excellent match between simulated and measured values of resonant frequency. For other two antennas too, the deviation between simulated and measured values of resonant frequency is in the order of 1.0–1.2%, which may be due possible air gap between the radiating patch and the dielectric material used. However, these deviations are well within tolerable limits and are well accepted for practical considerations. The deviations between simulated and measured values of resonant frequencies for antennas 4 and 5 are 0.0043% and 0.019% respectively, which are again well within acceptable limits for practical applications. The ripples exhibited by measured S_{11} result(s) may be due to the possible presence of few metallic obstructions in the Field Of View (FOV) of the antenna under test. As far as the impedance bandwidth is concerned, measured value of impedance bandwidth in each of these cases covers the entire HiperLAN/2 band and therefore these antennas can be designed and employed for High Performance Local Area Network applications.

4. FAR-FIELD RADIATION CHARACTERISTICS

4.1. Radiation Patterns (Simulated and Measured Results)

To study the radiation characteristics, at least two antennas are considered; one from the group of Copper based antennas and the next from electro-textile based group of antennas. Total far-field radiation patterns of electromagnetically modeled antennas 3, in both principal planes of $\phi = 0°$ (x-z) and $\phi = 90°$ (y-z), are obtained at its corresponding simulated resonant frequency of 5.8 GHz. Fabricated triangular microstrip antenna (# 3) is subjected to far-field radiation pattern measurements at its corresponding measured resonant frequency (5.775 GHz) in a rectangular shielded anechoic chamber. Simulated and measured far-field patterns of this triangular shaped wearable antenna (# 3) are shown in Figs. 7(a)–

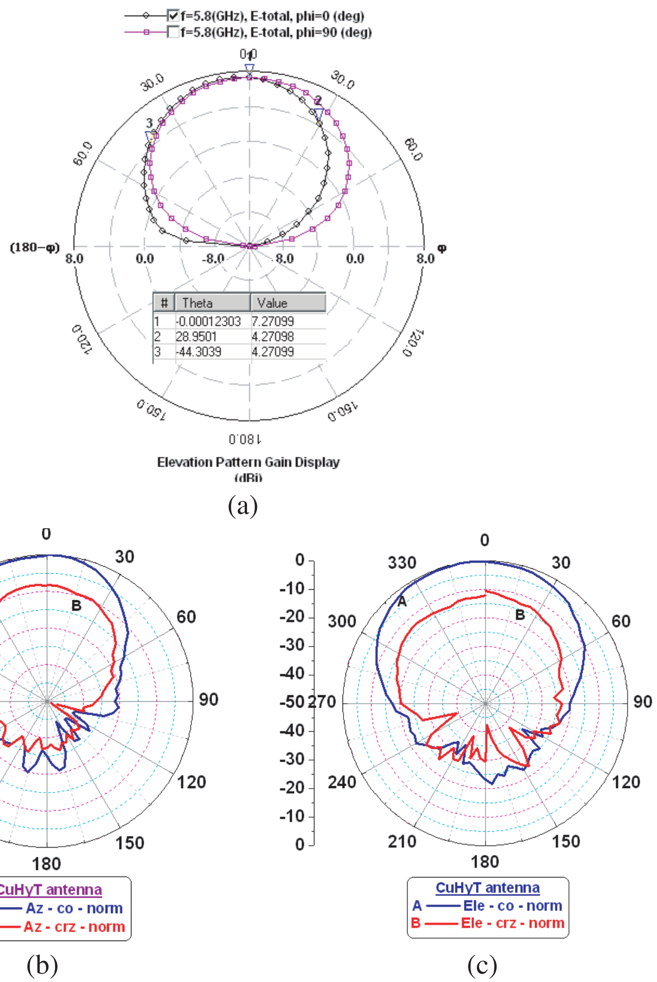

Figure 7. (a)–(c) Radiation patterns of triangular shaped wearable HiperLAN antenna.

(c). Referring to radiation patterns of the fabricated antenna (# 3), it is understood that the values of discrimination between co-polar and cross polar components in azimuth and elevation planes are 8.5 dB and 12.19 dB respectively. These values are reasonably good for practical applications. Simulated values of 3 dB beam-width in the x-z and y-z planes of this antenna are 73.25° and 83.09° respectively. Measured 3 dB beam-width values in azimuth and elevation planes, as obtained from the corresponding radiation pattern plots, are 77° and 73°.

Total far-field radiation patterns of electromagnetically modeled antenna (# 5), in both principal planes of $\phi = 0°$ (x-z) and $\phi = 90°$

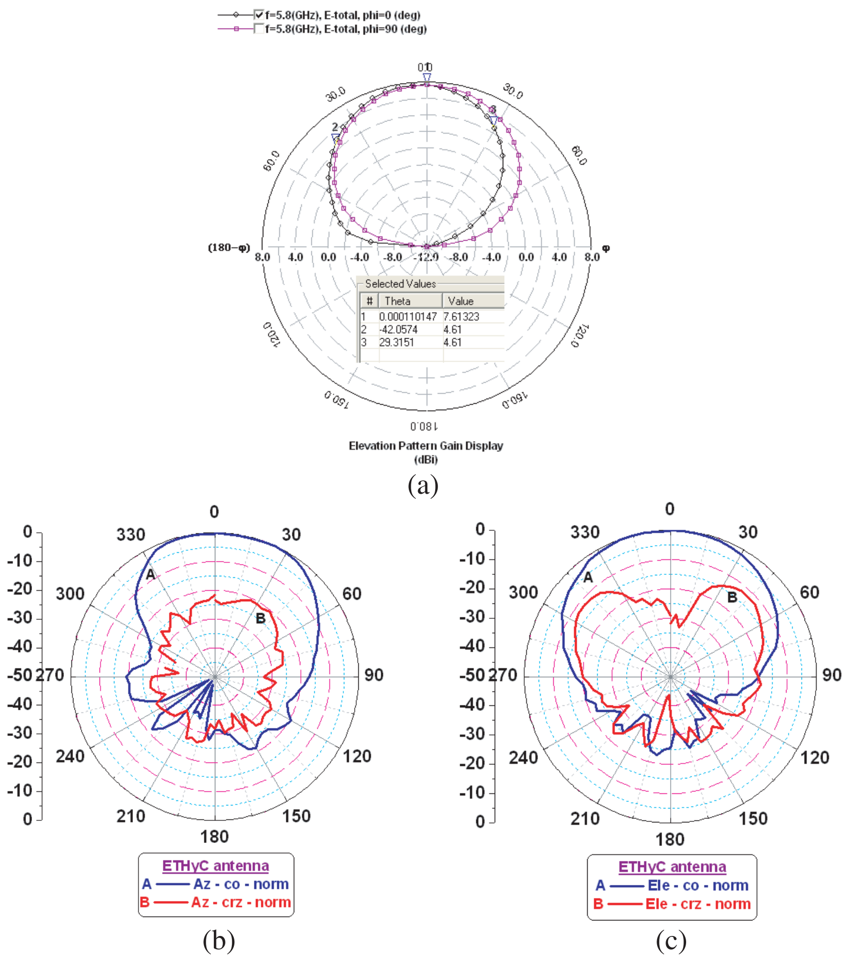

Figure 8. (a)–(c) Radiation patterns of antenna 5.

(y-z), are obtained at its simulated resonant frequency of 5.8 GHz. Fabricated circular microstrip antenna (# 5) is subjected to far-field radiation pattern measurements at its measured resonant frequency. Simulated and measured far-field patterns of this circular shaped wearable antenna (# 5) are shown in Figs. 8(a)–(c). Referring to radiation patterns of this antenna, it is understood that the values of discrimination between co-polar and cross polar components in azimuth and elevation planes of the fabricated wearable antenna (# 5) are 23.44 dB and 28.7 dB respectively. These values are reasonably good for practical applications. Simulated values of 3 dB beamwidth in the principal planes of this antenna are 71.38° and 78.31° respectively. Measured 3 dB beam-width values in azimuth and elevation planes, as obtained from the corresponding radiation pattern plots, are 70° and 73° respectively.

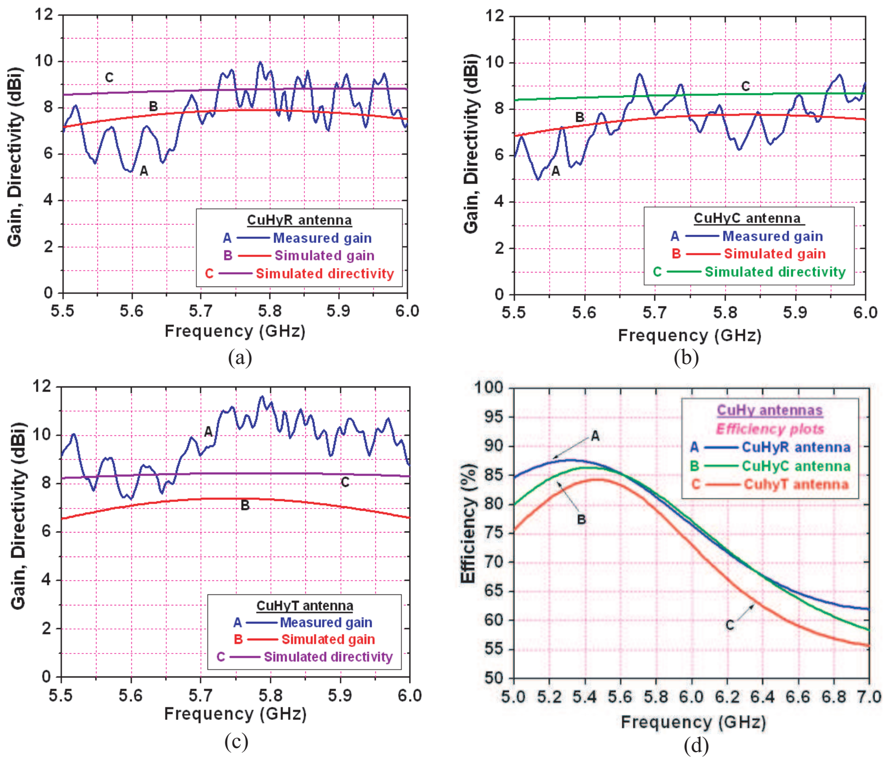

Figure 9. (a) Gain and directivity plots of antenna 1. (b) Gain and directivity plots of antenna 2. Gain and directivity plots of antenna 3. (d) Efficiency plots of antennas 1–3.

4.2. Gain, Directivity and Efficiency

Simulations are done for a range of frequencies from 5.5 GHz to 6.0 GHz in order to find antenna parameters like gain, directivity and radiating efficiency of all five antennas. Gain of each of these antennas in the same frequency range is measured using gain-comparison method [12]. Variations of simulated gain, measured gain and simulated directivity as functions of frequency for the investigated copper based antennas 1–3 are plotted in Figs. 9(a)–(c). The simulated radiating efficiency plots of these three antennas under study are shown in Fig. 9(d). In a similar fashion, variations of simulated gain, measured gain and simulated directivity as functions of frequency for the investigated antennas 4-5 are plotted in Figs. 10(a)–(b). The simulated radiating efficiency

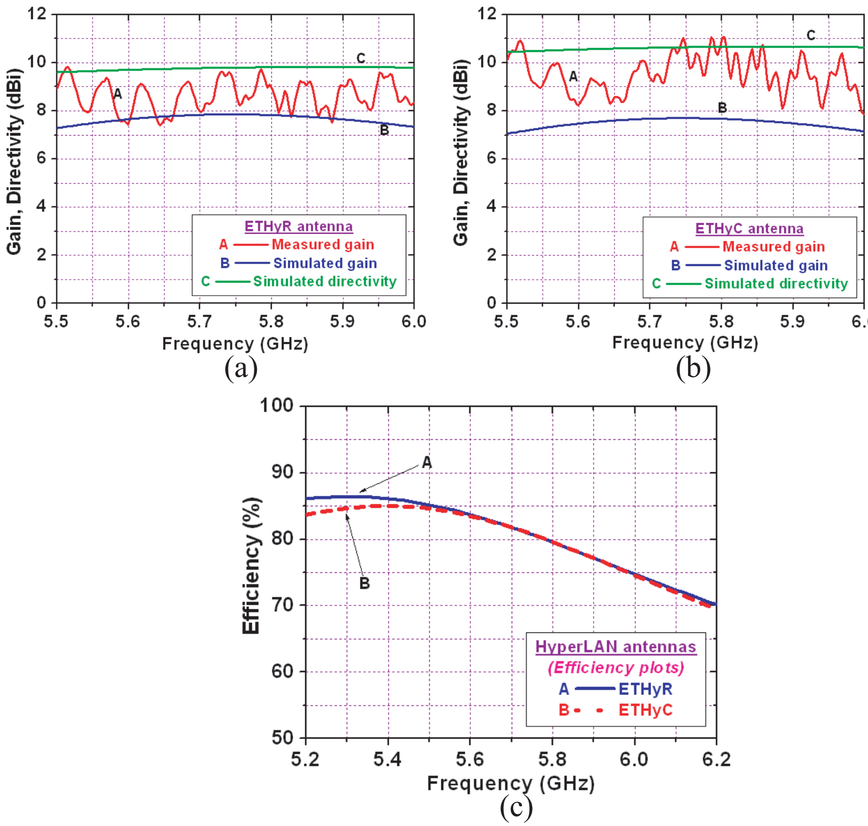

Figure 10. (a) Gain and directivity plots for antenna 4. (b) Gain and directivity plots for antenna 5. (c) Efficiency plots for antenna 4 and 5.

Table 3. Performance characteristics of HiperLAN wearable antennas.

Parameter	Antenna 1	Antenna 2	Antenna 3	Antenna 4	Antenna 5
Simulated gain (dBi)	7.91	7.78	7.35	7.85	7.67
Measured gain (dBi)	9.29	6.9	11.01	9.75	11.04
Simulated efficiency (%)	81.32	81.87	79.07	80.07	80.10
Simulated directivity (dBi)	8.82	8.66	8.44	9.82	10.66

plots of these two antennas under study are shown in Fig. 10(c). The measured values of directivity of antenna 3 and 5, which are subjected to radiation pattern measurements, are computed from measured radiation patterns using the standard formulae [12]. The performance characteristics of all these five antennas 1–5 are tabulated in Table 3. The characteristics exhibited by the developed antennas are very useful for practical considerations.

5. CONCLUSIONS

In this research work, five numbers of HiperLAN antennas with different geometries have been tested — three of them are with Copper based designs and the remaining two antennas are electro-textile based. All the five antennas are closely tuned to the designed resonant frequency and are giving good performance characteristics in terms of impedance bandwidth, gain, directivity, 3 dB beam-width and radiating efficiency. By testing these five antennas in this phase of work, it has been found that microstrip antenna is a suitable candidate for wearable applications as (1) it can be built using only fabric materials and (2) it can be made conformal to any shape. It is also understood that these antennas are very versatile and it is easy to make them operate at various frequency bands. Moreover, the well known techniques [9] of improving bandwidth and obtaining different polarizations, adopted for microstrip patch antennas are readily applied for these wearable antennas too. It may be concluded that this type of antenna may eventually replace the patch antennas on standard PCB substrates for various applications. The textile antennas must be drapable as the fabrics can take diverse shapes. Hence the bending effects on the performance characteristics of these antennas are to be taken into account when they are designed for wearable applications. The authors have already studied these phenomena with WLAN antennas, as reported in [5]. Moreover, the interaction between the wearable antenna and the human body can never be avoided and therefore, it requires further investigations.

ACKNOWLEDGMENT

The authors would like to thank Prof. P. Mohanan (Cochin University of Science and Technology, India), and Dr. T. Balakrishnan (Centre for Airborne Systems, Defence Research and Development Organization, India) for the help with the measurement of radiation pattern and gain; V. P. Sarin, R. Sujith, G. Prabhu Shankar, and Sanjay Manzhi for the assistance during antenna pattern measurements; Vishal Gupta (Agilent Technologies, New Delhi, India) and A. Senthil (Agilent Manufacturers' Representative, Chennai, India) for the constructive suggestions.

REFERENCES

1. Salonen, P. and L. Hurme, "A novel fabric WLAN antenna for wearable applications," *Proceedings of IEEE Antennas and Propagation Society International Symposium*, Vol. 2, 700–703, Jun. 2003.
2. Salonen, P. and H. Hurme, "Modeling of a fabric GPS Antenna for Wearable Applications," *Proceedings of IASTED International Conference Modeling and Simulation*, Vol. 1, 18–23, 2003.
3. Tanaka, M. and J. H. Jang, "Wearable microstrip antenna," *Proceedings of IEEE Antennas and Propagation Society International Symposium and URSI North American Radio Science Meeting*, Columbus, OH, USA, Jun. 2003.
4. Sankaralingam, S. and B. Gupta, "A novel technique for determination of dielectric constant of fabric materials for wearable antennas," *Proceedings of International Conference on Near-Field Characterization and Imaging (ICONIC)*, Vol. 1, 247–250, Taipei, Taiwan, Jun. 2009.
5. Sankaralingam, S. and B. Gupta, "Development of textile antennas for body wearable applications and investigations on their performance under bent conditions," *Progress In Electromagnetics Research B*, Vol. 22, 53–71, 2010.

6. Sankaralingam, S. and B. Gupta, "Performance study of a blue tooth antenna for wearable applications," *Proceedings of International Symposium on Antennas and Propagation (ISAP)*, Vol. 1, Bangkok, Oct. 2009.
7. Sankaralingam, S. and B. Gupta, "A circular disk microstrip WLAN antenna for wearable applications," *Proc. of IEEE India Conference (INDICON)*, Vol. 1, 513–516, Ahmedabad, India, Dec. 2009.
8. Sankaralingam, S. and B. Gupta, "A bluetooth antenna for on-body communications," *Proceedings of the Fourth European Conference on Antennas and Propagation (EuCAP)*, Barcelona, Spain, Apr. 2010.
9. Garg, R. and P. Bhartia, *Inder Bahl and Apisak Ittipiboon, Microstrip Antenna Design Handbook*, Artech House Publishers, 2001.
10. IE3D Electromagnetic Simulator from Zeland Software Inc., USA, Release 10.12, 2004.
11. Internet resources, Applying Error Correction to Network Analyzer Measurements, Agilent application note 5965-7709E, Mar. 27, 2002, Available: http://www.home.agilent.com.
12. Kraus, J. D., R. J. Marhefka, and A. S. Khan, "Antennas for all applications," 3rd edition, 24–25, Tata McGraw-Hill Publishing Company Ltd., New Delhi, 2006.